Immunocyte Ca^{2+} Influx System Mediated by LTRPC2

Yorikata Sano,*† Kohei Inamura,* Akira Miyake, Shinobu Mochizuki, Hiromichi Yokoi, Hitoshi Matsushime, Kiyoshi Furuichi

We characterized an activation mechanism of the human LTRPC2 protein, a member of the transient receptor potential family of ion channels, and demonstrated that LTRPC2 mediates Ca^{2+} influx into immunocytes. Intracellular pyrimidine nucleotides, adenosine 5′-diphosphoribose (ADPR), and nicotinamide adenine dinucleotide (NAD), directly activated LTRPC2, which functioned as a Ca^{2+}-permeable nonselective cation channel and enabled Ca^{2+} influx into cells. This activation was suppressed by intracellular adenosine triphosphate. These results reveal that ADPR and NAD act as intracellular messengers and may have an important role in Ca^{2+} influx by activating LTRPC2 in immunocytes.

Ca^{2+} influx functions as a trigger for the immune responses in immunocytes. The Ca^{2+} influx system has been studied extensively for its role in T cell receptor/CD3 complex–mediated Ca^{2+} influx in T lymphocytes (*1*–*5*). However, other Ca^{2+} influx in T lymphocytes and other immunocytes cannot be fully explained in terms of known components that influence Ca^{2+} influx.

Members of the transient receptor potential (TRP) channel family may represent additional Ca^{2+} influx components (*6*–*9*). These channels have been suggested as capacitative Ca^{2+} influx channels on the basis of a secondary structure. This channel family was first characterized as *Drosophila* TRP, and many mammalian homologs have been characterized and sorted, on the basis of their sequence similarity, into three TRP channel subfamilies: short (STRP), long (LTRP), and osm-9-like (OTRP) (*7*, *10*, *11*). Although the STRP and OTRP channel subfamilies have been clearly described, the LTRP channel subfamily is less well characterized but has been proposed to function as a component of the Ca^{2+} influx in immunocytes (*7*). In humans, three members of the LTRP channel subfamily, LTRPC1 (MLSN1), LTRPC2 (TRPC7), and LTRPC5 (MTR1), have been identified (*12*–*14*). The activation mechanism and characterization of one member, mouse TRP-PLIK, was recently reported (*15*); its in vivo functions are unclear, however.

We examined human LTRP channel family members as potential components mediating Ca^{2+} influx in immunocytes. To decide which channel of this family is expressed in human immunocytes, we performed reverse transcriptase polymerase chain reaction (RT-PCR) analysis of these members with mRNA from various human tissues, including peripheral blood. LTRPC2 is expressed abun-

Molecular Medicine Laboratories, Institute for Drug Discovery Research, Yamanouchi Pharmaceutical Co., Ltd., 21 Miyukigaoka, Tsukuba, Ibaraki 305–8585, Japan.

*These authors contributed equally to this work.
†To whom correspondence should be addressed. E-mail: sano.yorikata@yamanouchi.co.jp

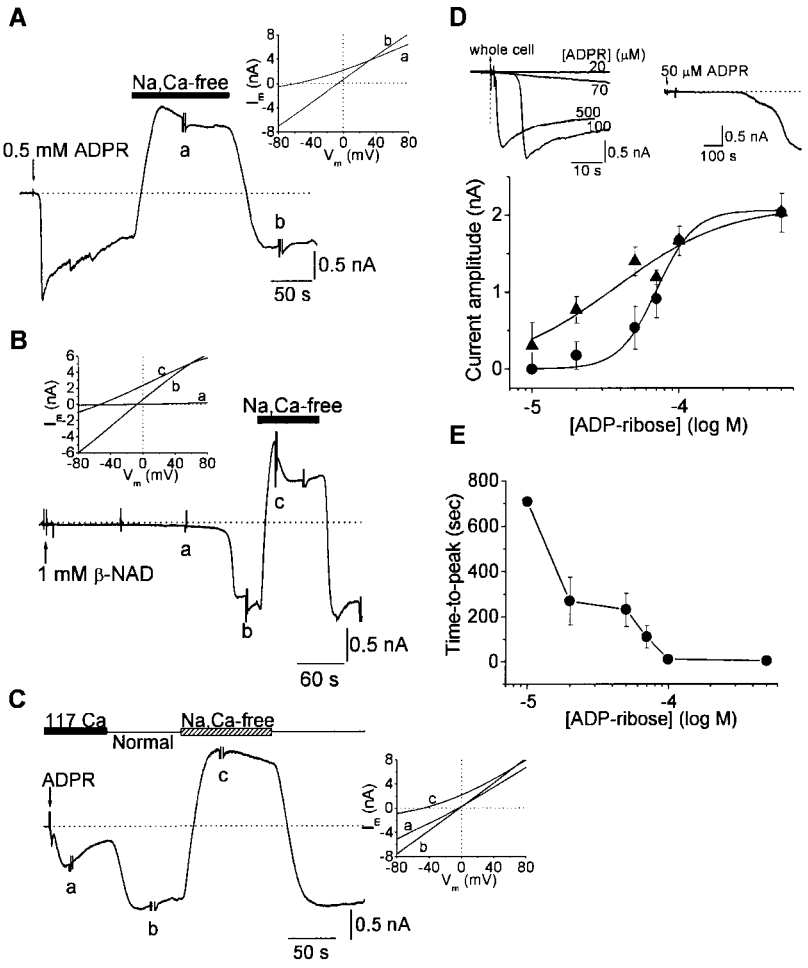

Fig. 1. The activation of LTRPC2 by intracellular ADPR and β-NAD. (**A**) Dialysis of 0.5 mM ADPR induces a response in LTRPC2-expressing HEK293 cells. The holding potential was –15 mV. The upper bar indicates the replacement of normal solution with Na^+,Ca^{2+}-free solution. The dotted line indicates the zero current level. The inset shows the I-V relations recorded by applying a voltage ramp from –80 to +80 mV (50 mV/s) at the response for the (a) Na^+,-Ca^{2+}-free or (b) normal solutions. The arrow indicates the break into the whole-cell mode. (**B**) The response to β-NAD in LTRPC2-expressing HEK293 cells. The holding potential was –15 mV. The upper bar indicates the replacement of normal solution with Na^+,Ca^{2+}-free solution. The inset shows the I-V relations. a, before, and b, during the response in normal solution; c, Na^+,Ca^{2+}-free solution. (**C**) The response to ADPR in isotonic 117 mM Ca^{2+} solution. The holding potential was –15 mV. The upper bar indicates the replacement of solutions. The inset shows the I-V relations. a, Th^{117} with Ca^{2+}; b, normal; and c, Na^+,Ca^{2+}-free solutions. (**D**) Dose-response relations for ADPR at 3 min (circles) and 20 min (triangles) after the formation of the whole-cell configuration. The curves show the best fit to the data with the Hill equation and give values for I_{max} of 2.1 and 2.1 nA, $K_{1/2}$ of 70 and 40 μM, and n of 3.4 and 1.1, respectively. The insets show the ADPR-induced inward currents at different concentrations. The concentrations are expressed at the top of each trace. (**E**) Kinetics of the ADPR-induced currents plotted as a function of ADPR concentrations.

dantly in peripheral blood, and the channel is expressed in some blood cell lines (*16*, *17*). Prediction of protein-sorting signals and localization sites (PSORT) analysis indicated that LTRPC2 has seven transmembrane domains, and a motif database (BLOCKS database) search revealed a MutT motif in the cytoplasmic COOH-terminal region. The MutT motif has been reported to participate in hydrolase activity toward nucleotides (*16*–*19*).

On the basis of these studies, we examined whether various nucleotides—α-NAD, β-NAD, the reduced form of NAD^+ (NADH), adenosine monophosphate, adenosine diphosphate, ADPR, ribose, or ribose 5′-phosphate—activated LTRPC2 in whole-cell patch-clamp experiments with LTRPC2-expressing human embryonic kidney (HEK) 293 cells, in which LTRPC2 is not expressed endogenously (*16, 17*, *20*, *21*). Of these nucleotides, intracellular dialysis of only ADPR and β-NAD evoked an inward current after membrane rupture in all the cells examined (Fig. 1, A and B). No such currents were observed in HEK293 cells that did not express LTRPC2 during the test interval of 30 min after membrane rupture when the internal solution in the pipette contained ADPR or β-NAD. Moreover, changes in the membrane potential of LTRPC2-expressing cells did not cause channel openings. Although the response to ADPR occurred immediately, the onset of the response to β-NAD began 441 ± 91 s (n = 8) after membrane rupture (Fig. 1B). The current-voltage (*I-V*) relation was examined by applying a voltage ramp at the response in normal or Na^+,Ca^{2+}-free solutions. The slope of the *I-V* curve measured during the response in normal solution was almost linear, indicating a lack of voltage dependency. The mean reversal potential was estimated to be –4.3 ± 0.4 mV (n = 9), which was similar to the potential for the response to β-NAD (–5.3 ± 1.4 mV, n = 8). Moreover, the average reversal potentials measured with KCl and CsCl pipette solutions in LTRPC2-expressing L929 (murine fibrosarcoma) cells gave similar values (–0.6 mV). In the Na^+,Ca^{2+}-free solution, the average reversal potentials of responses to ADPR and β-NAD measured with CsCl pipette solution were estimated to be –55.1 ± 2.4 mV (n = 8) and –56.0 ± 2.0 mV (n = 6), respectively. In addition, the replacement of most of Cl^- with gluconate did not shift the reversal potential (–10 ± 0.8 mV, n = 5). Thus, LTRPC2 appears to be a nonselective cation channel that permits equal permeation of Na^+, K^+, and Cs^+ but excludes Cl^-.

To study the Ca^{2+} permeability of LTRPC2, we activated currents in the presence of isotonic 117 mM $CaCl_2$ solution. After dialysis of ADPR under these conditions, ADPR caused a prominent inward current (Fig. 1C). The reversal potential of the ADPR-induced response did not shift compared to that under normal conditions (Fig. 1C). The average value was –2.0 ± 1.7 mV (n = 4) and the permeability ratio P_{Ca}/P_{Cs} was 0.67. Thus, LTRPC2 functions as a Ca^{2+}-permeable nonselective cation channel.

The magnitude of the inward current induced by ADPR depended on the concentration of ADPR added and plateaued at a concentration of ADPR >100 μM (Fig. 1D). A delayed response was observed at a low concentration of ADPR (Fig. 1D). Because no response to ADPR was observed in the control HEK293 cells after 20 min (n = 5), this late response reflects LTRPC2 channel activities. In fact, the time-to-peak value from membrane rupture increased with an increase in the ADPR concentration (Fig. 1E).

Because it was demonstrated that β-NAD–induced activation is slower than that by ADPR, it is possible that β-NAD is metabolized into ADPR by cytoplasmic and/or membrane components. To investigate the former possibility, we tested β-NAD and ADPR in inside-out patches that were excised from LTRPC2-expressing HEK293 cells and applied directly to LTRPC2 without cytoplasmic components. The perfusion of ADPR and β-NAD in the bath solution induced channel activities instantaneously and reversibly (Fig. 2, A and B). The single-channel *I-V* relation for the channel activated by ADPR was outward rectification with a unitary conductance of 58 pS at negative potentials and 76 pS at positive potentials, and it reversed at 0 mV (Fig. 2C). The properties of the single-channel *I-V* relation for the β-NAD–induced response were indistinguishable from those for the ADPR-induced response (Fig. 2C).

To investigate the latter possibility, we examined the effect of CD38, which is a membrane component and has an activity for metabolizing β-NAD to ADPR (*22*, *23*). CD38 is endogenously expressed in HEK293 cells but is not expressed in L929 cells (Fig. 2D) (*24*). We examined the β-NAD–induced activation of LTRPC2 in inside-out patches excised from LTRPC2-expressing L929 cells. The application of β-NAD instantaneously induced the activation of LTRPC2, and this activation was not different from that in LTRPC2-expressing HEK293 cells (Fig. 2E). These results indicate that ADPR and β-NAD directly activate LTRPC2 without cytoplasmic or membrane components.

In U937 cells, the monocyte cell lines in which LTRPC2 was abundantly expressed, intracellular dialysis of ADPR and β-NAD into cells elicited responses (Fig. 3, A to C). Similarly, with LTRPC2-expressing HEK-293 cells, the onset of the β-NAD–induced current was significantly later than that of the

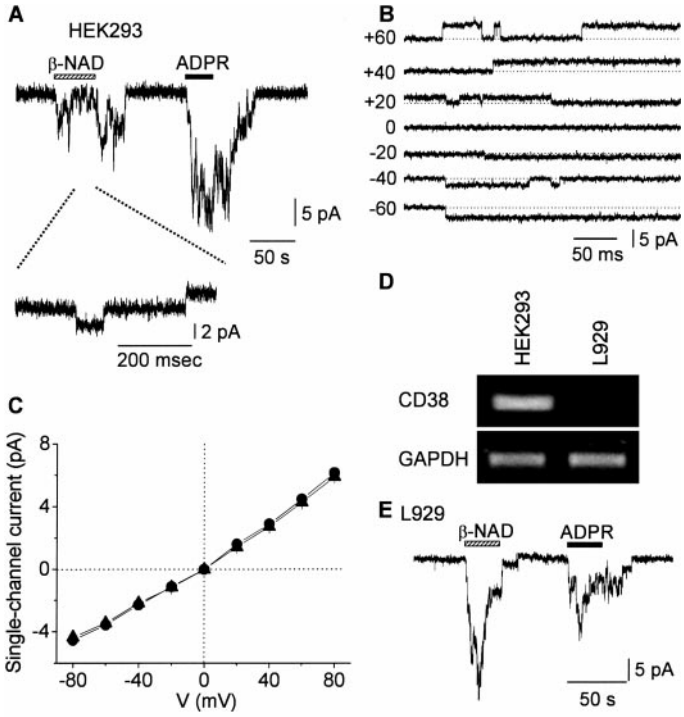

Fig. 2. Direct activation of LTRPC2 by ADPR and β-NAD. (**A**) Multichannel currents activated by ADPR and β-NAD in an inside-out patch excised from LTRPC2-expressing HEK293 cells. The holding potential was –40 mV. The recording pipette contained the normal external solution, and the bath solution contained 150 mM KCl and 2 mM $MgCl_2$. The upper bars indicate periods of stimulation. (**B**) Single-channel currents of LTRPC2 activated by ADPR at different membrane potentials obtained in inside-out patches. Dotted lines denote the closed state. (**C**) Single-channel *I-V* relations for LTRPC2 activated by ADPR (circles) and β-NAD (triangles). A linear regression yielded a slope conductance of 58 pS at negative potentials and 76 pS at positive potentials. (**D**) RT-PCR analysis for CD38 with total RNA of HEK293 and L929 cells. (**E**) Multichannel currents activated by ADPR and β-NAD in an inside-out patch excised from LTRPC2-expressing L929 cells. The holding potential was –40 mV. The upper bars indicate periods of stimulation.

ADPR-induced current (Fig. 3D). Moreover, a Ca^{2+} current was observed in isotonic $CaCl_2$ solution (*25*). We also observed ADPR-induced currents in EOL1 cells (eosinophilic cell lines) and Jurkat cells (T lymphocyte cell lines), which were correlated with the expression level of LTRPC2 (Fig. 3E) (*17*). These results indicate that ADPR- and β-NAD–induced currents in U937 cells are mediated via LTRPC2. Furthermore, it is indicated that these currents mediated by the activation of LTRPC2 are not only in U937 but in Jurkat and EOL1, that is, widely in immunocytes.

These findings suggest a novel Ca^{2+} influx system mediated by ADPR and β-NAD–induced activation of LTRPC2, but the regulation mechanism of LTRPC2 for activation in immunocytes remains unclear, because β-NAD exists abundantly in living cells (*26*) and dialysis of β-NAD induced a significantly later inward current than that of ADPR. Moreover, β-NAD instantaneously and directly activated LTRPC2 in inside-out patches. The activation of the *Drosophila* TRP channel depends on intracellular adenosine triphosphate (ATP) concentrations (*27*). Thus, we tested whether ATP could regulate the activation of LTRPC2. In an inside-out patch in which the channels were activated with β-NAD, the addition of ATP together with β-NAD resulted in decreased channel activity (Fig. 4, A and C), whereas the addition of ATP with ADPR slightly reduced the response (Fig. 4, B and C). These results suggest that β-NAD–induced activation of LTRPC2 may be regulated by intracellular ATP. Because ATP constitutively exists in normal cells, it is suggested that β-NAD–induced activation may be suppressed by intracellular ATP under normal conditions. Thus, the likely reason for the delay in whole-cell responses to β-NAD (Fig. 1, B and D) is that the ATP concentration is decreased or depleted by washing out during the process of patch-clamp experiments.

We have demonstrated a novel Ca^{2+} influx system, mediated by LTRPC2, in immunocytes. In addition, in this system, we showed that the intracellular pyrimidine nucleotides ADPR and NAD appear to act as intracellular messengers for the Ca^{2+} influx in immunocytes. Although NAD is abundant in cells, intracellular concentrations of ADPR are regulated by the membrane component CD38 (*22*, *23*). This ADPR production is accelerated by ATP depletion (*28*). Thus, we propose two Ca^{2+} influx systems: (i) ADPR is produced by CD38 during ATP depletion and directly activates LTRPC2; and (ii) NAD directly activates LTRPC2 when ATP is depleted, and activated LTRPC2 causes Ca^{2+} influx into cells. Moreover, NAD causes apoptosis in Jurkat cells (*29*). Our results suggest that in vivo LTRPC2 may link apoptosis with the metabolism of ADPR and NAD.

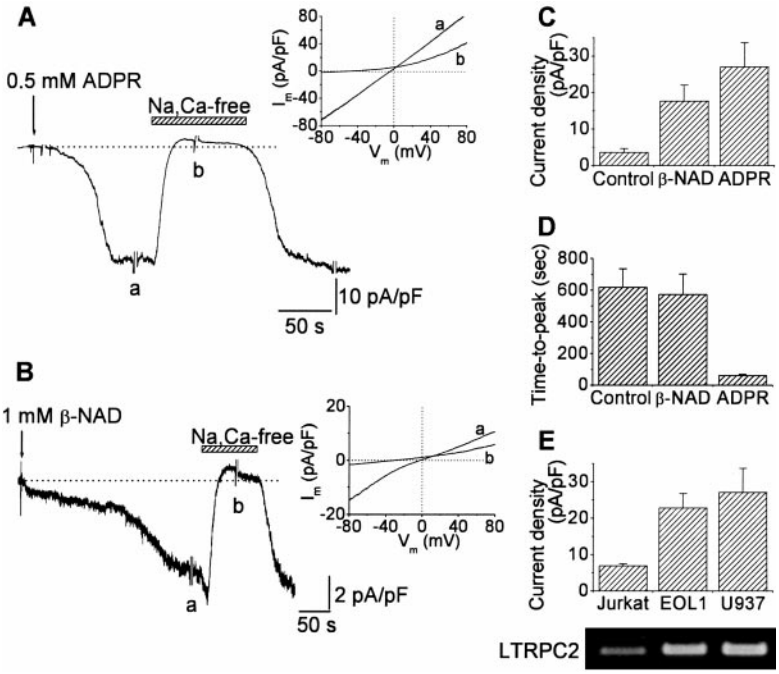

Fig. 3. Cationic current in monocyte cell lines induced by ADPR and β-NAD. (**A**) Trace of whole-cell current induced by dialysis of ADPR in U937 cells at a holding potential of −40 mV. The upper bar indicates the replacement of normal solution with Na^+,Ca^{2+}-free solution. The inset shows the I-V relations recorded by applying a voltage ramp from −80 to +80 mV at the response in (a) normal or (b) Na^+,Ca^{2+}-free solutions. (**B**) Trace of whole-cell current induced by dialysis of β-NAD in U937 cells at a holding potential of −40 mV. The upper bar indicates the replacement of normal solution with Na^+,Ca^{2+}-free solution. The inset shows the I-V relations recorded by applying a voltage ramp. (**C**) Current densities of ADPR- and β-NAD–induced responses in U937 cells. (**D**) Time-to-peak values of the ADPR- and β-NAD–induced currents. (**E**) Current densities of ADPR-induced response in Jurkat, EOL1, and U937 cells, and RT-PCR analysis for LTRPC2 with total RNA of these cell lines. The 660–base pair fragments were amplified.

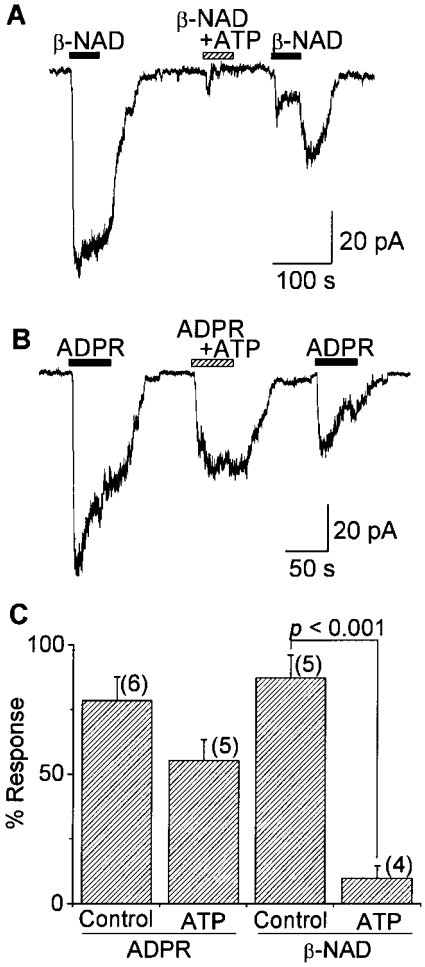

Fig. 4. The suppression of LTRPC2 by intracellular ATP. (**A**) Representative trace of the responses to β-NAD alone and the addition of 1 mM ATP/2Na^+ together with β-NAD recorded at an inside-out patch containing multichannels. The upper bars indicate periods of stimulation. The response to β-NAD with ATP was strikingly decreased compared with the response to β-NAD alone. (**B**) Representative trace of the responses to ADPR alone and the addition of 1 mM ATP/2Na^+ together with ADPR. The upper bars indicate periods of stimulation. (**C**) Effects of ATP (1 mM) on currents induced by ADPR and β-NAD. To quantify the inhibition effect in a situation when currents decline spontaneously, we measured the ratios of the test stimulation (second application) to the average value of first and third stimulation. The control was measured in the absence of ATP. The response to β-NAD was significantly different from the control level when data were analyzed by Student's *t* test ($P < 0.001$). The response to ADPR was slightly affected ($P = 0.048$). The number of experiments is given in parentheses.

References and Notes

1. A. H. Guse, *Crit. Rev. Immunol.* **18**, 419 (1998).
2. _____, *J. Mol. Med.* **78**, 26 (2000).
3. A. Weiss, *Annu. Rev. Genet.* **25**, 487 (1991).
4. T. H. Finkel, R. T. Kubo, J. C. Cambier, *Immunol. Today* **12**, 79 (1991).
5. A. Weiss, R. D. Littman, *Cell* **76**, 263 (1994).
6. J. W. Putney Jr., R. R. McKay, *Bioessays* **21**, 38 (1999).
7. C. Harteneck, T. D. Plant, G. Schultz, *Trends Neurosci.* **23**, 159 (2000).
8. T. Hofmann, T. Schaefer, G. Schultz, T. Gudermann, *J. Mol. Med.* **78**, 14 (2000).
9. L. Missiaen *et al.*, *Cell Calcium* **28**, 1 (2000).
10. B. T. Bloomquist *et al.*, *Cell* **54**, 723 (1988).
11. C. Montell, G. M. Rubin, *Neuron* **2**, 1313 (1989).
12. L. M. Duncan *et al.*, *Cancer Res.* **58**, 1515 (1998).
13. K. Nagamine *et al.*, *Genomics* **54**, 124 (1998).
14. D. Prawitt *et al.*, *Hum. Mol. Genet.* **9**, 203 (2000).
15. L. W. Runnels, L. Yue, E. D. Clapham, *Science* **291**, 1043 (2001).
16. The RT reaction was carried out with random hexamer primers included in the Advantage RT Kit (Clontech, Palo Alto, CA). PCR primers (5′- TCTCCGGCG-CAGCAACAGCA-3′and 5′-CCCTCGCGGCGGTGGA-CAGT-3′) were designed from the human LTRPC2 mRNA sequence (GenBank accession number AB001535) and used to amplify a 660-nucleotide fragment from human multiple mRNA and blood cell lines total RNA.
17. Supplementary figures are available on *Science* Online at www.sciencemag.org/cgi/content/full/293/5534/1327/DC1.
18. M. J. Bessman, D. N. Frick, S. F. O'Handley, *J. Biol. Chem.* **271**, 25059 (1996).
19. M. Wilding, L. G. Russo, A. Galione, M. Marino, B. Dale, *Am. J. Physiol.* **275**, C1277 (1998).
20. LTRPC2 cDNA was cloned by RT-PCR with oligonucleotide primers. The polyadenylated RNA was isolated from human lymphocytes and the first-strand cDNA was synthesized with the Advantage RT kit. The cDNA was amplified by PCR by means of the primers, and the amplified DNA was cloned into pcDNA3.1 vector (Invitrogen, Carlsbad, CA). HEK293 and L929 cells were transfected with LTRPC2 cDNA for electrophysiological studies, as described [A. Miyake, S. Mochizuki, H. Yokoi, M. Kohda, K. Furuichi, *J. Biol. Chem.* **274**, 25018 (1999); S. Mochizuki, A. Miyake, K. Furuichi, *Amino Acids* **17**, 243 (1999)]. Cells were cotransfected with the LTRPC2 expression vector described previously and the green fluorescent protein expression vector phGFP S65T (Clontech) by the transfection reagent FuGENE6 (Roche Diagnostics, Mannheim, Germany), and cultured in Dulbecco's modified Eagle's medium supplemented with 10% fetal bovine serum. Transfected cells were identified by observing GFP fluorescence with an epifluorescence microscope. Electrophysiological studies were carried out 2 to 3 days after transfection.
21. Electrophysiological recordings were performed from LTRPC2 transfectants by means of a voltage-clamp technique [O. P. Hamill, A. Marty, E. Neher, B. Sakmann, F. J. Sigworth, *Pflugers Arch.* **391**, 85 (1981)]. Recordings were made with an Axopatch 1D amplifier (Axon Instruments, Foster City, CA) by means of patch electrodes with a resistance of 3 to 10 megohms. Single-channel recording data were filtered at 2 kHz and sampled at 20 kHz. The internal pipette solution contained 150 mM CsCl, 5 mM $MgCl_2$, and 10 mM Hepes-Cs (pH 7.2). The external solution contained 145 mM NaCl, 5 mM KCl, 2 mM $CaCl_2$, 2 mM $MgCl_2$, and 10 mM Hepes-Na (pH 7.4). The Na^+,Ca^{2+}-free solution contained 150 mM *N*-methyl-D-glucamine, 2 mM $MgCl_2$, and 10 mM Hepes [pH 7.4 (adjusted with HCl)]. For the inside-out patch experiments, the recording pipette contained the normal external solution, and the bath solution contained 150 mM KCl, 2 mM $MgCl_2$, and 10 mM Hepes-K (pH 7.4). For the calcium permeability experiments, the bath solution was changed to 117 mM $CaCl_2$ and 5 mM Hepes [pH 7.4 (adjusted with $Ca(OH)_2$)] after the establishment of a gigohm seal with the recording pipette containing 135 mM CsCl, 4.5 mM EGTA, and 9 mM Hepes-Cs (pH 7.2). The low Cl^- solution contained 145 mM Na gluconate, 5 mM K gluconate, 2 mM $CaCl_2$, 2 mM $MgCl_2$, and 10 mM Hepes-Na (pH 7.4). Ca permeability was calculated relative to Cs by the Goldman-Hodgkin-Katz modified constant field equation [C. A. Lewis, *J. Physiol.* **286**, 417 (1979)]. All recordings were performed at room temperature (25°C). Analysis was carried out on a personal computer with pCLAMP software (Axon Instruments). All values are expressed as means ± SEM. Statistical significance was tested with Student's *t* test. No corrections were made for junction potentials. All reagents were purchased from Sigma. The ATP was 2 Na^+ salt.
22. M. Howard *et al.*, *Science* **262**, 1056 (1993).
23. K. Mehta, U. Shahid, F. Malavasi, *FASEB J.* **10**, 1408 (1996).
24. For the RT-PCR analysis in Fig. 2D, the RT reaction was carried out with random hexamer primers included in the Advantage RT Kit. PCR primers were designed from human and mouse CD38 mRNA sequences.
25. Y. Sano *et al.*, unpublished data.
26. S. Sestini, G. Jacomelli, M. Pescaglini, V. Micheli, G. Pompucci, *Arch. Biochem. Biophys.* **379**, 277 (2000).
27. K. Agam *et al.*, *J. Neurosci.* **20**, 5748 (2000).
28. I. Kato *et al.*, *J. Biol. Chem.* **270**, 30045 (1995).
29. M. K. Han, Y. S. Cho, Y. S. Kim, C. Y. Yim, U. H. Kim, *J. Biol. Chem.* **275**, 20799 (2000).

30. We thank J. Ishikawa,. T. Saito, M. Kawamura, and C. Kitada for helpful comments and K. Tsunoyama for bioinformatic analysis and helpful comments. We also thank A. Matsuo for technical assistance.

14 May 2001; accepted 19 June 2001

The Role of *Drosophila* Mushroom Body Signaling in Olfactory Memory

Sean E. McGuire,[1] Phuong T. Le,[1] Ronald L. Davis[1,2]*

The mushroom bodies of the *Drosophila* brain are important for olfactory learning and memory. To investigate the requirement for mushroom body signaling during the different phases of memory processing, we transiently inactivated neurotransmission through this region of the brain by expressing a temperature-sensitive allele of the *shibire* dynamin guanosine triphosphatase, which is required for synaptic transmission. Inactivation of mushroom body signaling through α/β neurons during different phases of memory processing revealed a requirement for mushroom body signaling during memory retrieval, but not during acquisition or consolidation.

In the insect, distinct brain structures termed the mushroom bodies (MBs) play a central role in associative learning of olfactory information (*1*, *2*). The MBs of *Drosophila melanogaster* comprise about 2500 neurons per brain hemisphere (Fig. 1). The cell bodies of these neurons are situated in the dorsal posterior brain region and extend axons anteriorly and ventrally through the peduncle to give rise to the α/β, α′/β′, and γ lobes (*3*–*6*). These lobes are neuropil regions that contain the MB cell axons and other processes that synapse with MB neurons.

Genetic and chemical disruption of the MBs produces flies that are normal for general behaviors but are defective in olfactory learning (*7*, *8*). Many genes involved in olfactory learning and memory show enriched expression in the MBs, particularly those encoding components of the cyclic adenosine monophosphate signaling pathway (*2*). Targeting of a constitutively active G-protein α subunit to the MBs disrupts olfactory learning (*9*), and restoring the *rutabaga*-encoded adenylyl cyclase specifically to the MBs of *rutabaga* mutants is sufficient to restore short-term memory in these flies (*10*). The model that has emerged from these experiments posits the MBs as important centers in olfactory associative learning and the likely site of convergence of the conditional (CS) and unconditioned (US) stimuli in classical conditioning (*1*, *2*, *11*).

A limitation of the previous experiments is that they all involve permanent alterations to the fly's brain throughout development, leading to the possibility that some of the effects on learning might reflect developmental perturbations rather than modifications of the physiology of these neurons that subserve learning and memory processes. Additionally, the irreversible nature of these interventions has made it impossible to dissect the roles of the MBs at the different stages of memory acquisition, consolidation, and retrieval.

To explore the roles of the MBs in the different phases of memory processing, we used an approach that allows us to transiently inactivate synaptic transmission from the MBs by targeting expression of a temperature-sensitive *shibire*^{ts1} transgene to the MBs by the GAL4/UAS system (*12*, *13*). The *shibire* gene encodes a dynamin guanosine triphosphatase (GTPase) that is essential for synaptic vesicle recycling (*14*, *15*) and maintenance of the readily releasable pool of synaptic vesicles (*16*). The temperature-sensitive

[1]Department of Molecular and Cellular Biology and [2]Department of Psychiatry and Behavioral Sciences, Baylor College of Medicine, Houston, TX 77030, USA.

*To whom correspondence should be addressed. E-mail: rdavis@bcm.tmc.edu